



Angiotensin II type 2 receptor as a novel activator of brown adipose tissue in obesity

Fabiola Alvarez-Gallego¹ | Raquel González-Blázquez² | Marta Gil-Ortega² |
 Beatriz Somoza² | María Calderón-Dominguez^{3,4} | Javier Moratino⁵ |
 Virginia Garcia-Garcia⁵ | Paloma Fernández⁵ | Daniel González-Moreno² |
 Marta Viana¹  | Martín Alcalá¹ 

¹Departamento de Química y Bioquímica, Facultad de Farmacia, Universidad San Pablo-CEU, CEU Universities, Boadilla del Monte, Madrid, Spain

²Departamento de Ciencias Farmacéuticas y de la Salud, Facultad de Farmacia, Universidad San Pablo-CEU, CEU Universities, Boadilla del Monte, Madrid, Spain

³Biomedical Research and Innovation Institute of Cadiz (INiBICA) Research Unit, Puerta del Mar University Hospital, Cádiz, Spain

⁴Biomedicine, Biotechnology and Public Health Department, University of Cadiz, Cádiz, Spain

⁵Instituto de Medicina Molecular Aplicada Nemesio Díez, Universidad San Pablo-CEU, CEU Universities, Boadilla del Monte, Madrid, Spain

Correspondence

Martín Alcalá and Marta Viana, Facultad de Farmacia, Universidad San Pablo-CEU, Ctra. Boadilla del Monte Km 5.300, 28925, Alcorcón, Madrid, Spain.

Email: martin.alcaladiazmor@ceu.es and mvana@ceu.es

Abstract

The angiotensin II type 2 receptor (AT2R) exerts vasorelaxant, anti-inflammatory, and antioxidant properties. In obesity, its activation counterbalances the adverse cardiovascular effects of angiotensin II mediated by the AT1R. Preliminary results indicate that it also promotes brown adipocyte differentiation in vitro. Our hypothesis is that AT2R activation could increase BAT mass and activity in obesity. Five-week-old male C57BL/6J mice were fed a standard or a high-fat (HF) diet for 6 weeks. Half of the animals were treated with compound 21 (C21), a selective AT2R agonist, (1 mg/kg/day) in the drinking water. Electron transport chain (ETC), oxidative phosphorylation, and UCP1 proteins were measured in the interscapular BAT (iBAT) and thoracic perivascular adipose tissue (tPVAT) as well as inflammatory and oxidative parameters. Differentiation and oxygen consumption rate (OCR) in the presence of C21 was tested in brown preadipocytes. In vitro, C21-differentiated brown adipocytes showed an AT2R-dependent increase of differentiation markers (*Ucp1*, *Cidea*, *Pparg*) and increased basal and H⁺ leak-linked OCR. In vivo, HF-C21 mice showed increased iBAT mass compared to HF animals. Both their iBAT and tPVAT showed higher protein levels of the ETC protein complexes and UCP1, together with a reduction of inflammatory and oxidative markers. The activation of the AT2R increases BAT mass, mitochondrial activity, and reduces markers of tissue inflammation and oxidative stress in obesity. Therefore, insulin reduction and better vascular responses are achieved. Thus,

Abbreviations: ADRF, adipocyte-derived relaxing factor; Ang II, angiotensin II; AT1R, angiotensin II type 1 receptor; AT2R, angiotensin II type 2 receptor; C21, compound 21; DM, differentiation medium; ETC, electron transport chain; HF, high-fat; iBAT, interscapular brown adipose tissue; lncRNA, long non-coding RNA; mBA, mouse brown preadipocytes; OCR, oxygen consumption rate; oxPhos, oxidative phosphorylation; RAS, renin-angiotensin system; SOD, superoxide dismutase; tPVAT, thoracic perivascular adipose tissue; UCP1, uncoupling protein 1; WAT, white adipose tissue; β -AR, beta adrenergic receptor.

Fabiola Alvarez-Gallego, Raquel González-Blázquez, Marta Viana, and Martín Alcalá contributed equally to this work.

This is an open access article under the terms of the [Creative Commons Attribution](https://creativecommons.org/licenses/by/4.0/) License, which permits use, distribution and reproduction in any medium, provided the original work is properly cited.

© 2023 The Authors. *BioFactors* published by Wiley Periodicals LLC on behalf of International Union of Biochemistry and Molecular Biology.

Funding information

Ministerio de Ciencia e Innovación,
Grant/Award Number:
PID2020-114343GA-I00; Universidad San
Pablo CEU - Banco Santander,
Grant/Award Numbers: FUSP-BS-PPC-
USP03/2017, FUSP-PPC-19-C5B625BA

the activation of the protective arm of the renin–angiotensin system arises as a promising tool in the treatment of obesity.

KEYWORDS

AT2R, brown adipose tissue, compound 21, electron transport chain, perivascular adipose tissue, UCP1

1 | INTRODUCTION

Although traditionally characterized as a thermogenic organ,^{1,2} brown adipose tissue (BAT) is currently recognized as an active agent that collaborates to maintain metabolic homeostasis beyond body temperature regulation. BAT activity has been associated with lower risk of type 2 diabetes, dyslipidemia, coronary artery disease, cerebrovascular disease, heart failure, and hypertension. These outcomes were supported by lower blood glucose, triglyceride, and HDL values and overall suggested its potential as a treatment against metabolic diseases.³

The underlying mechanisms for these metabolic improvements lie in three key features of brown adipocytes: (1) an elevated fuel (both glucose and fatty acids) uptake rate together with a high mitochondrial density that facilitates substrate clearance from circulation⁴; (2) adaptive, non-shivering thermogenesis, conferred by the uncoupling protein 1 (UCP1), a proton channel within the inner mitochondrial membrane. UCP1 uncouples the energy generated by the respiratory chain from the production of ATP, dissipating it as heat⁵; and (3) an important role as a secretory organ, releasing different factors that regulate glucose and lipid metabolism such as batokines, lncRNA, or lipid mediators.^{6–9}

In mice, interscapular BAT (iBAT) is the most abundant brown adipose depot, and it has been widely studied due to its fuel oxidation and thermogenic capacity. However, the discovery of its properties as an endocrine organ opened a new window for the study of the inter-organ crossed communication. Based on these observations, the activation of peripheral and minor depots such as thoracic perivascular adipose tissue (tPVAT), cardiac, and perirenal BAT, which may not have a significant impact on energy expenditure, have demonstrated important roles in the regulation of nearby organs.^{10,11} For instance, the activation of tPVAT releases bioactive molecules that regulate the aortic function.¹² In addition, vascular injury promotes tPVAT browning, triggering a compensatory mechanism to regulate the inflammatory response, contributing to a protective vascular remodeling.¹³

The regulation of BAT activity by adrenergic stimulation has been widely studied. In mice, BAT is activated by the sympathetic nervous system via β 3-adrenergic

receptor (β 3-AR), which enhances UCP1 transcription and activity and stimulates lipolysis.^{14–16} However, the translation to humans is controversial. On the one hand, the use of sympathomimetics increases the risk of suffering side effects, especially those related with the cardiovascular system. On the other hand, the presence of β 3-AR in brown adipocytes has not been fully proven yet¹⁷ so the beneficial metabolic effects of high doses of β 3-AR agonist mirabegron¹⁸ could, in fact, reflect the result of an off-target activation of β 1-AR and β 2-AR receptors.¹⁷ Because of these concerns, identifying new activators (including natriuretic peptides,¹⁹ hormones and bile acids, capsaicins and capsinoids, and catechins,²⁰ among others) becomes highly relevant in the use of BAT as a therapeutic tool.

In this context, recent evidence points at the reparative branch of the renin angiotensin system (RAS) as a potential BAT activator. Angiotensin II (Ang II), the main bioactive peptide in the RAS system, binds with the same affinity to the Ang II type 1 (AT1R) and type 2 (AT2R) receptors. AT1R, which is highly and ubiquitously expressed, promotes vasoconstriction, fibrosis, and inflammation. On the other side, AT2R is the main member of the reparative branch of the RAS system. This receptor is also ubiquitous, but it is lowly expressed in physiological conditions.²¹ When activated, it exerts the opposite effects to AT1R, including vasorelaxation and prevention of hypertrophy, fibrosis, and inflammation,²² which are typical features of the obese BAT.²³ There is evidence that the components of the RAS are also present in the adipose tissue and that both Ang II and AT1R levels are overactivated in obesity, participating in the pathogenesis of this disease.²⁴ Interestingly, AT2R activation with Ang II²⁴ or Ang 1–7^{24,25} promotes browning of white adipose tissue (WAT). Furthermore, the administration of a non-peptide AT2R agonist, Compound 21 (C21), also promoted browning of WAT and brown adipogenesis²⁴ in lean animals.

The aim of this study was to determine if the activation of the reparative branch of the RAS has the capacity to enhance the function of the BAT in order to be used as a therapeutic tool in the treatment of obesity. We hypothesize that the activation of AT2R in a mice model of diet-induced obesity could increase both the mass and the

activity of the BAT, arising as a new mechanism of activation with potential applications in metabolic diseases. According to our results, the oral administration of C21 for 6 weeks was able to increase iBAT mass and to overstimulate the mitochondrial respiration and uncoupling capacity in obese mice. The anti-inflammatory and antioxidant effects are, at least partially, responsible for the enhanced biological activity of both iBAT and tPVAT, which may account for the metabolic and vascular improvements observed in these animals.

2 | EXPERIMENTAL PROCEDURES

2.1 | Animals

Four-week-old male C75BL/6 J mice inbred at Universidad San Pablo-CEU animal facilities were used for this experiment. Mice were maintained in our facility to acclimatize for 1 week prior to the experiments under controlled light (12:12 h light–dark cycles), temperature (22–24°C), and relative humidity (44%–55%) with access to standard food and water. Animals were then divided into two groups and fed ad libitum for 6 weeks with either chow diet (CHOW: Teklad Rodent Diet 2918, 18% of Kcal from fat, 58% of Kcal from carbohydrates, and 24% of Kcal from proteins; 3.1 kcal/g) supplied by Envigo (USA) or High Fat diet (HF: D12451, 62% of Kcal from fat, 20% of Kcal from carbohydrates, and 18% of Kcal from proteins; 5.1 kcal/g) supplied by Test Diet (UK). Simultaneously, half of the animals of each group were treated with the non-peptide specific AT2R agonist C21 (1 mg/kg/day in drinking water, Vicore Pharma), generating four different groups: CHOW-C, CHOW-C21, HF-C, and HF-C21. C21 is a non-peptide AT2R-specific agonist with an oral bioavailability of 30%. It has a K_i value of 0.4 nM for the AT2R and a $K_i > 10$ μ M for the AT1R. Body weight was monitored twice a week and water consumption was daily recorded to readjust the dose of C21 accordingly.

The vascular effects of this experimental approach have been previously reported in González-Blázquez et al.^{26,27} The experimental procedures were performed in accordance with the European Union Laboratory Animal Care Rules (86/609/ECC directive) and approved by the Ethical Committee of the San Pablo CEU University and the Animal Protection Area of the Comunidad Autónoma de Madrid (PROEX 200/18).

After 6 weeks of diet and treatment, mice were weighed and euthanized at 9 a.m. by decapitation. After iBAT and tPVAT excision, an aliquot was snap frozen in liquid nitrogen and stored at –80°C and another aliquot was immersed in 4% paraformaldehyde (PFA) for histological analysis.

2.2 | Metabolic parameters

Plasma glucose was determined by an enzymatic colorimetric test (GOD-PAP, Roche Diagnostics, Barcelona, Spain). Plasma levels of insulin were measured using the Mouse Insulin Elisa kit (Mercodia, Denmark).

2.3 | Histological analysis

BAT samples were preserved in a 4% PFA for 24 h and then transferred to 70% ethanol. The specimens were then paraffin-embedded, cut into 4- μ m sections and stained with hematoxylin and eosin. The area occupied by lipid droplets was quantified using ImageJ software 1.53 (NIH, USA). Macrophage infiltration was evaluated by CD68 immunostaining (Mouse CD68/SR-D1 Antibody, 1/300, Bio-Techne R&D Systems, USA). Briefly, tissue sections were deparaffinized and antigen retrieval was performed after 20 min of citrate unmasking at 95°C. BOND polymer refine detection system was used in an automated Leica BOND-III system (both from Leica, Germany) for the detection of antigen-bond primary antibodies. The stained slides were scanned with the Leica Aperio Versa system (20 \times) and analyzed with the Leica Aperio ImageScope 12.4.

2.4 | Cell culture experiments

An immortalized line of mouse brown preadipocytes cell line (mBA) was generated and kindly provided by Dr Ángela M. Valverde from the Alberto Sols Biomedical Research Institute. Cells were cultured in Dulbecco's modified Eagle's medium (DMEM) with 2 mM L-glutamine (L-0102, Biowest, France), 10% FBS (Biowest, France), penicillin/streptomycin (100 U/mL) (Gibco), and HEPES and maintained at 37°C in a humidified atmosphere containing 5% CO₂ until 80% confluence was reached. The cells were differentiated into mature brown adipocytes in a 7-day process. A total of 75,000 cells/mL were seeded in culture plates with the differentiation medium (DM) supplemented with 20 nM insulin (Merck Life Science, USA) and 1 nM 3,3',5'-triiodo-L-thyronine (T3) (Merck Life Science, USA). After 24 h (day 0), the DM was changed to an induction medium (IM) supplemented with 0.5 μ M dexamethasone (Sigma), 1 μ M rosiglitazone (Sigma), 0.125 μ M indomethacin and 0.5 mM 3-isobutyl-1-methylxanthine (Sigma). After 2 days, the medium was replaced by DM and changed every 2 days to avoid nutrient deprivation. On the last day, cells have achieved their mature conformation, which becomes obvious due to the numerous lipid

droplets and their round shape. To study the role of C21 in preadipocytes differentiation process, cells were treated with 100 nM C21 or in combination with prior treatment with AT2R antagonist PD123319 (100 nM, 20 min) or AT1R antagonist losartan (100 nM, 20 min).

2.5 | Oil red O staining

Oil red O solution was prepared by diluting stock solution (3 mg/mL, Sigma-Aldrich-Merck, USA) in 2:3 ratio with distilled water for 10 min and then filtered. Cultured cells were washed with PBS and fixed with a 10% PFA solution for 30 min. After washing with distilled water, 60% isopropanol solution was added for 5 min to permeabilize the cells and removed. The diluted red oil solution was added to the cells and incubated in dark condition for 15 min. Cells were finally washed five times with distilled water and analyzed in an inverted microscope (Eclipse TS100, Nikon, UK).

2.6 | Western blot analysis

Frozen iBAT and tPVAT was homogenized in protein extraction buffer (NaCl [0.42 M], $\text{Na}_4\text{PO}_2\text{O}_7$ [1 mM], DTT [10 mM], HEPES [0.02 M], sodium orthovanadate [1 mM], EDTA [1 mM], EGTA [1 mM], glycerol 20%, PMSF [2 mM], leupeptine [0.001 mg/mL], aprotinin [0.001 mg/mL], TLCK [0.001 mg/mL], triton X-100 [1%]). For cell culture experiments, cells were collected with RIPA buffer directly from the culture dish. Protein concentration was determined (Pierce BCA Assay Kit, Thermo-Fisher Scientific, USA) and 30 μg of protein were loaded. Samples were separated on 10% SDS-PAGE gels and then transferred onto 0.45 μm PVDF membranes (BioRad). The following primary antibodies were incubated overnight at 4°C: UCP1 (anti-UCP1 antibody, ab10983, 1/5000; Abcam, UK), mitochondrial complexes I, II, III, IV, and V (OxPhos Rodent WB Antibody Cocktail, 45–8099, 1/5000; Life Technologies, USA), AT1 (anti-AT1 antibody, ab124734, 1/1000, Abcam, UK), AT2 (anti-AT2 antibody, ab92445, 1/1000; Abcam, UK), tubulin (α -tubulin, 11H10, 1/1000, Cell Signalling, USA), GAPDH (anti-GAPDH antibody, G8795, 1/5000, Merck Life Science, USA). Blots were incubated with the appropriate IgG-HRP-conjugated secondary antibody. Protein bands were visualized using the ECL immunoblotting detection system (GE Healthcare) and developed on ChemiDoc XRS + Imaging System (BioRad, Hercules, CA). For the analysis of protein expression, bands were quantified by densitometry using Image Lab analysis software. Results were normalized by tubulin or GAPDH and expressed as % of control.

2.7 | Analysis of mRNA expression by quantitative real-time PCR

Total RNA was isolated from iBAT, tPVAT, and brown adipocytes using Illustra RNspin Mini (GE Healthcare) following the manufacturer instructions; 500 ng of RNA was reverse transcribed to cDNA using 5 \times PrimeScript™ RT-PCR Kit (Takara Bio, Japan). Relative gene expression was analyzed in 6.25 ng of cDNA using 500 nM forward and reverse primers (listed in Supplementary Table S1) and 2 \times TB Green Premix Ex Taq (Tli RNase H Plus) (Takara Bio, Japan) in a CFX96 Thermocycler (BioRad, USA). The $-\Delta\Delta\text{Ct}$ method was used to calculate the relative gene expression. In the cell culture experiments, *Tbp* and *Actb* were used as housekeeping genes and the expression of the undifferentiated cells at day 0 was set as 1. In iBAT and tPVAT, *Hprt1* and *Gapdh* were selected as housekeeping genes, and the relative expression of the CHOW group was set as 1.

2.8 | Oxygen consumption rate

Brown preadipocytes grown to 80% confluence from a t75 cell culture flask were plated into eight-well cell culture miniplates (Agilent) and differentiated into brown mature adipocytes following the previously described protocol. After differentiation, the real-time oxygen consumption rate (OCR) was assessed using the Seahorse XF HS Mini Extracellular Flux Analyzer (Agilent). On the day of the experiment, XF assay media supplemented with glucose (25 mM) was added to the differentiated brown adipocytes and maintained in a CO_2 -free incubator for 1 h. Basal OCR was initially recorded. After the injection of the ATPase inhibitor oligomycin (0.2 μM), proton leak and ATP-linked respiration were calculated. Next, the uncoupling agent FCCP (0.2 μM) was injected to analyze the maximal respiration rate. The spare respiratory capacity was calculated as the Maximal OCR – Basal OCR. Finally, a combination of the electron transport chain (ETC) inhibitors rotenone (1 μM) and antimycin A (1 μM) was injected to differentiate between the mitochondrial and the non-mitochondrial oxygen consumption. The non-mitochondrial OCR was subtracted to calculate the OCR parameters and the results were normalized to total protein content.

2.9 | Superoxide dismutase antioxidant enzyme activity

iBAT samples were homogenized in a buffer containing 50 mM Tris, pH = 7.4 and 5 mM EDTA. Superoxide

dismutase (SOD) activity assay is based on the inhibition of cytochrome C oxidation in the presence of superoxide generated by xanthine and xanthine oxidase. Briefly, 50 μL of the diluted sample was combined in a spectrophotometric cuvette with 1 mL of 50 mM phosphate buffer, pH = 7.8 at 37°C, 50 μL of 0.1 mM cytochrome C and 250 μL of 0.5 mM xanthine. The reaction was triggered by the addition of 50 μL of 0.02 U/mg protein of xanthine oxidase. The appearance of oxidized cytochrome C was continuously measured at 546 nm for 2 min. All the reagents were purchased from Sigma-Aldrich-Merck (USA).

2.10 | Statistical analysis

Data are shown as the mean values \pm standard error of the mean (SEM). All statistics were performed by Prism 9.0 (GraphPad). Data were tested for a normal (Gaussian) distribution using Shapiro–Wilk normality test. The presence of outliers was tested using the ROUT's test ($Q = 1\%$). Multiple comparisons were performed by using one-way factorial ANOVA or two-way repeated-measures

ANOVA followed by Tukey's post hoc test. p values less than 0.05 were considered statistically significant.

3 | RESULTS

3.1 | AT2R activation does not increase thermogenesis in mature brown adipocytes

To test the effect of AT2R activation on thermogenesis and brown differentiation in vitro, we used immortalized brown preadipocytes from C57BL/6J mice. The incubation with induction and differentiation media for 6 days led to mature brown adipocytes (Figure 1A). First, to confirm that this type of cell may respond to AT2R agonists, we quantified AT1R and AT2R by Western blot. AT1R was poorly detected in undifferentiated cells, while AT2R was undetectable. However, both receptors increased their expression during brown adipocyte differentiation, reaching prominent levels by day 6 (Figure 1B).

Once the presence of the two main receptors in the RAS system was established in mature brown adipocytes,

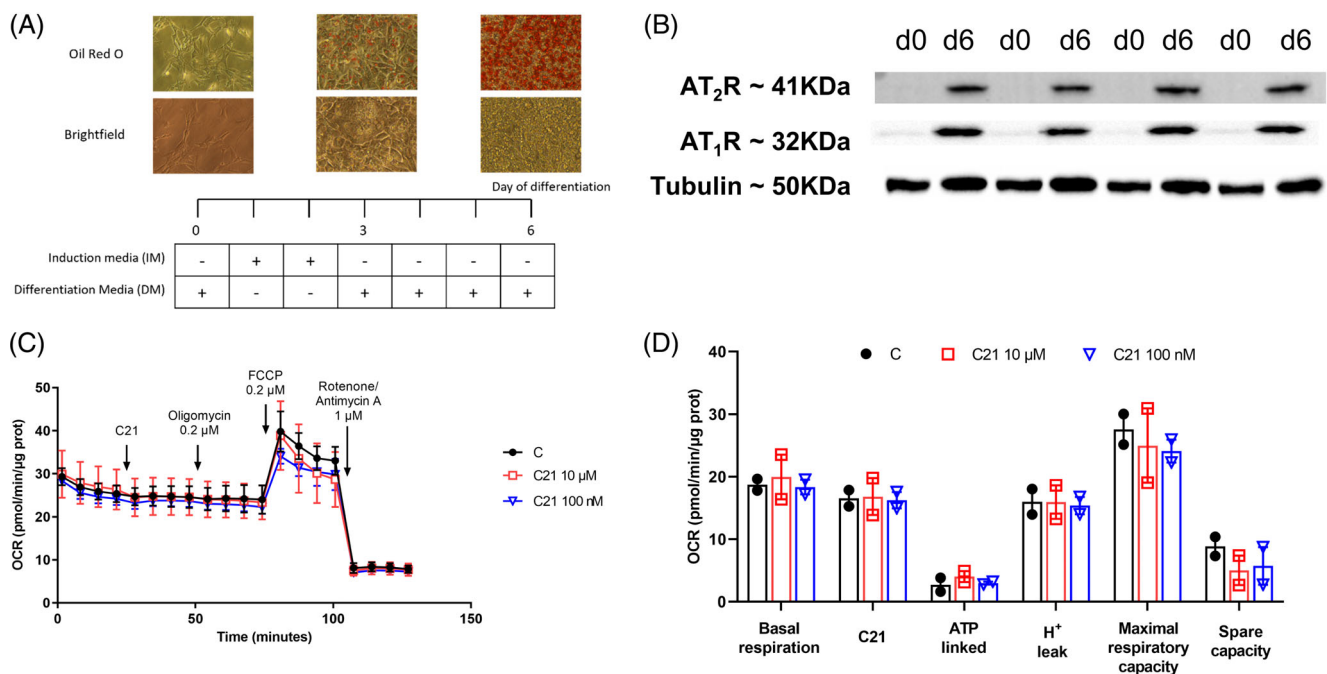


FIGURE 1 AT2R agonist C21 activates mouse brown adipocytes in a time-dependent manner. (A) Differentiation protocol of the immortalized mouse brown preadipocytes (day 0) to mature brown adipocytes (day 6). The adipogenic process was followed using the oil red O staining. (B) Representative immunoblots of protein levels for AT2R and AT1R at day 0 and day 6 of differentiation ($n = 4$). Tubulin levels were used as a loading control. (C) Bioenergetic profile of brown adipocytes (day 6) after the injection of two different concentrations of C21 (10 μM —red squares and 100 nM—blue triangles). Basal oxygen consumption rate (OCR) is first recorded. Then, C21 was added. After oligomycin was injected, ATP-linked respiration and proton leak were calculated. Maximal respiration and reserve capacity were measured after FCCP addition, and finally, ETC inhibitors were added to determine non-mitochondrial oxygen consumption. Concentration of inhibitors and incubation times are described in Section 2. Results are normalized by protein content ($n = 2$). (D) Bioenergetic parameters were calculated from the OCR traces. Data are represented as mean \pm SEM. AT2R, angiotensin II type 2 receptor; C21, compound 21; ETC: electron transport chain.

we wanted to test whether the incubation with C21, a selective AT2R agonist was able to induce thermogenesis. By means of a Seahorse, we injected two concentrations of C21 (10 μ M and 100 nM) after recording the basal OCR. We observed no response to any of the two tested doses (Figure 1C,D) in a continuous OCR measurement for 30 min. Other mitochondrial-related respiratory parameters (H^+ leak, ATP synthesis, maximal respiration, or spare capacity) also remained unaltered after the incubation with C21, suggesting that in our model, an acute injection of C21 does not increase mitochondrial activity in mature brown adipocytes.

3.2 | AT2R activation by C21 modulates brown differentiation in a dose-dependent manner

We next wanted to test if AT2R activation could enhance brown differentiation. To address this issue, we treated brown preadipocytes with C21 along the differentiation process (Figure 2A), observing a dose-dependent effect on brown adipocytes. When tested in the micromolar range (10 and 100 μ M), C21 inhibit brown differentiation as it can be inferred from the decreased expression of differentiation markers such as *Ucp1*, *Prdm16*, and *Cidea* (Figure 2B–D). However, when tested in the nanomolar range (100 nM), we found an upregulation of these markers after 6 days of cell differentiation (Figure 2E–G). In addition, specific AT1R and AT2R antagonists (losartan and PD123319, respectively) were used to demonstrate that the effect was AT2R specific, since it was abolished in cells pre-treated with PD123319 but not with losartan.

Finally, to test if the increase in brown adipocyte differentiation by 100 nM C21 is reflected in the thermogenic capacity, we analyzed the OCR using the same differentiation model described above (Figure 2H,I). From the beginning of the experiment, C21-differentiated adipocytes exhibited a high OCR ($p = 0.06$) in comparison to the adipocytes differentiated with the standard method. When oligomycin, an ATPase inhibitor, was injected, we observed a significant OCR increase in the C21-differentiated adipocytes without detecting changes in ATP-linked respiration. No changes in other parameters (maximal respiratory rate or spare capacity) were detected.

3.3 | Effect of HFD and C21 treatment on body weight, iBAT weight, and iBAT lipid accumulation

Next, we wanted to determine if the AT2R-mediated differentiation observed in vitro could account for metabolic

improvements in a mice model of diet-induced obesity. For 6 weeks, mice receiving a HF diet were administered 1 mg/kg of C21 in the drinking water. At sacrifice, both groups of animals fed on a HF diet showed an increased body weight in comparison to CHOW mice. C21 administration did not prevent body weight gain (Figure 3A). Circulating glucose levels were increased in both HF-fed groups compared to their corresponding controls, with no additional effects of the C21 treatment (Figure 3B). Insulin levels were also increased in the HF group compared to CHOW as a response to the elevated glucose levels. However, plasma insulin concentration in HF-C21 were significantly lower than in the HF group, suggesting that AT2R activation in obesity may participate in metabolic homeostasis by reducing insulin secretion (Figure 3C). The weight of iBAT was increased in HF mice compared to the control and it was even higher in those treated with C21 (Figure 3D), indicating hypertrophy of the tissue. A histological examination was performed to determine whether that increase in the mass was due to fat accumulation or brown adipocyte expansion. BAT from obese mice showed more unilocular adipocytes compared with the multilocular adipocytes present in CHOW mice (Figure 3E). Fat accumulation was indirectly quantified by estimating the percentage of the area occupied by lipid droplets. No differences were found between the two groups fed a HF diet (Figure 3F), suggesting that the increase of BAT mass in HF-C21 was due to an enhanced brown differentiation and proliferation rather than fat accumulation.

To evaluate the influence of HF diet and C21 in the expression of Ang II receptors in BAT, we measured the expression of AT1R and AT2R by Western blot. Protein levels of AT1R were increased in HF mice. However, treatment with C21 reverted this effect reaching the same expression level as the control group (Figure 3G). Protein levels of AT2R were also increased in the HF group in comparison to the CHOW group, but no effect of C21 treatment was observed (Figure 3H).

3.4 | C21 activates the ETC and uncoupling capacity in iBAT of obese mice

To evaluate whether AT2R activation may modulate mitochondrial oxidation capacity in the iBAT, protein levels of complexes I, II, III, IV, and V (ATP synthase) and UCP1 were measured by Western blot. HF diet significantly increased the levels of complexes I, II, III, IV, and UCP1, but not ATP synthase (Figure 4A–G). The concomitant administration of C21 with the HF diet promoted a further increase in the expression of complex III (Figure 4D) and UCP1 (Figure 4G) compared to the HF group.

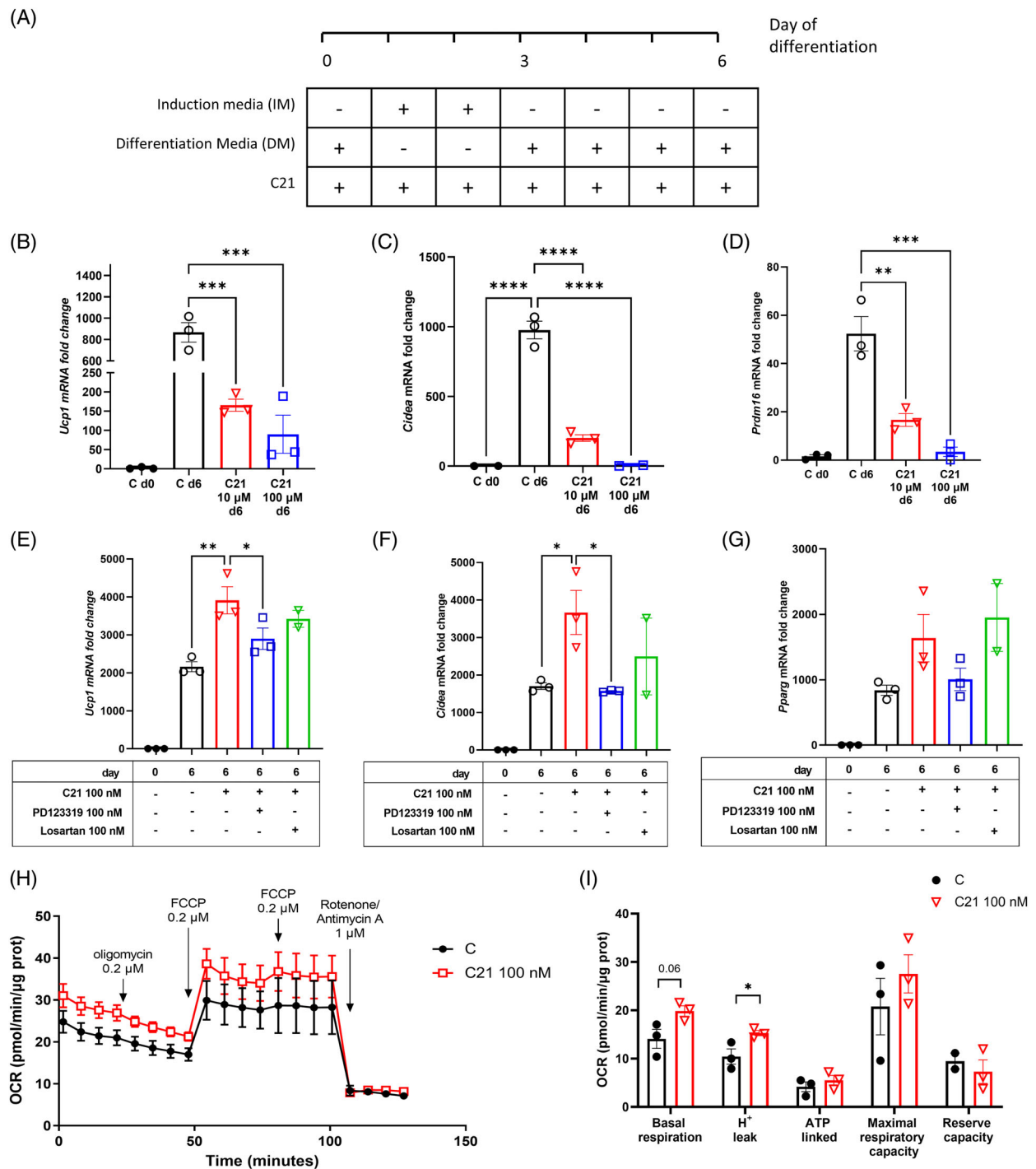


FIGURE 2 Dose-specific effect of C21 in brown adipocyte differentiation. (A) Differentiation protocol of the immortalized mouse brown preadipocytes (day 0) to mature brown adipocytes (day 6). First, brown preadipocytes were differentiated in the presence of C21 in the micromolar range (10 μ M and 100 μ M). mRNA levels of BAT differentiation markers were used to track the differentiation process: (B) *Ucp1*, (C) *Prdm16*, and (D) *Cidea*. The relative expression of the undifferentiated cells (day 0) was set as 1. Results were normalized using the expression of *Tbp* and *Actin* as housekeeping genes. Then, brown preadipocytes were differentiated in the presence of C21 in the nanomolar range (100 nM), using specific AT1R and AT2R antagonists (losartan, 100 nM, 20 min preincubation and PD123319, 100 nM, 20 min preincubation, respectively). mRNA levels of (E) *Ucp1*, (F) *Prdm16*, and (G) *Cidea* were measured. (H) Oxygen consumption rate of brown adipocytes (day 6) differentiated in the presence of 100 nM C21 from day 0. Oligomycin (ATP synthase inhibitor), FCCP (uncoupling agent), and a combination of Rotenone and Antimycin A (ETC inhibitors) were injected as described in the Section 2. (I) Bioenergetic parameters were calculated from the OCR traces: Basal respiration, proton leak, ATP-linked respiration, maximal respiration capacity, and reserve capacity. Data are represented as mean \pm SEM ($n = 3$). * $p < 0.05$, ** $p < 0.01$, *** $p < 0.001$, **** $p < 0.0001$. C21, compound 21; ETC: electron transport chain; OCR: oxygen consumption rate.

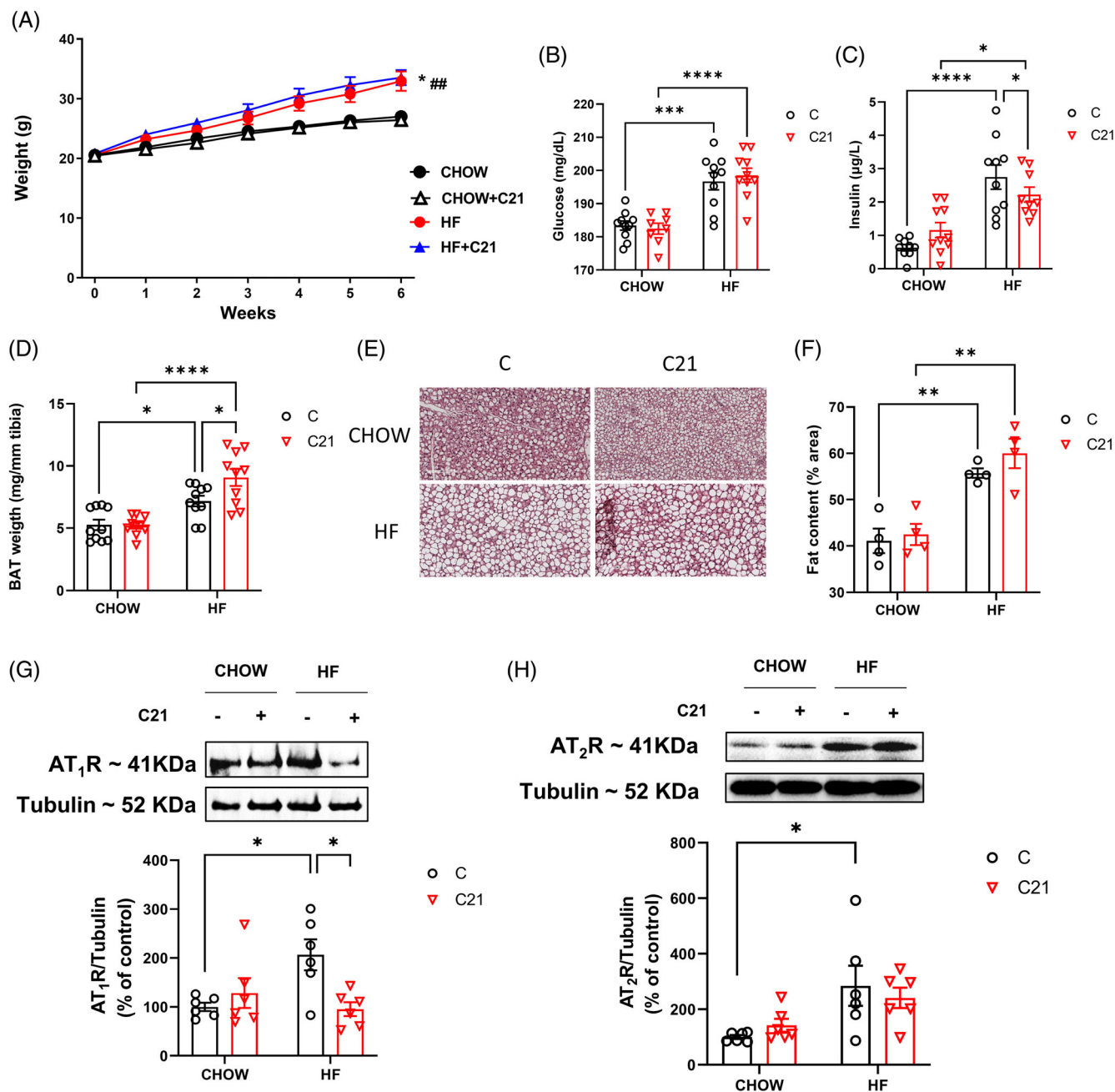


FIGURE 3 C21-mediated AT₂R activation increases iBAT mass and contributes to metabolic homeostasis in obese mice. C57BL/6/J male mice were fed on a Chow or HF diet for 6 weeks. Half of the animals received 1 mg/kg/day of C21 in the drinking water along the whole experiment. (A) Evolution of the body weight during the 6 weeks of treatment. Postprandial circulating levels of (B) glucose and (C) insulin. (D) iBAT weight, expressed as mg/mm tibia. (E) Representative images of hematoxylin/eosin stain of paraffin-embedded iBAT slices. (F) Quantification of fat inclusion within iBAT, measuring the % of the image occupied by lipid droplets and normalized by the total area. Relative protein levels of AT₁R (G) and AT₂R (H) in iBAT lysates. Tubulin levels were used as a loading control and the relative quantification of the Chow group was set as 100%. Data are represented as mean ± SEM. Experiments were performed with *n* = 6 mice per group. **p* < 0.05, ***p* < 0.01, ****p* < 0.001, *****p* < 0.0001. AT₂R, angiotensin II type 2 receptor; C21, compound 21; HF: high-fat; iBAT: interscapular brown adipose tissue.

The enhancement of the ETC and uncoupling capacity observed in the HF group may be linked to an increase in mitochondrial biogenesis, as it can be inferred from the increased expression of *Pgc1a* and *Mfn1* in comparison to

the CHOW group (Figure 4H,I). However, the additional activation caused by C21 in HF-fed animals was independent of mitochondrial biogenesis since both *Pgc1a* and *Mfn1* expression were similar to CHOW animals.

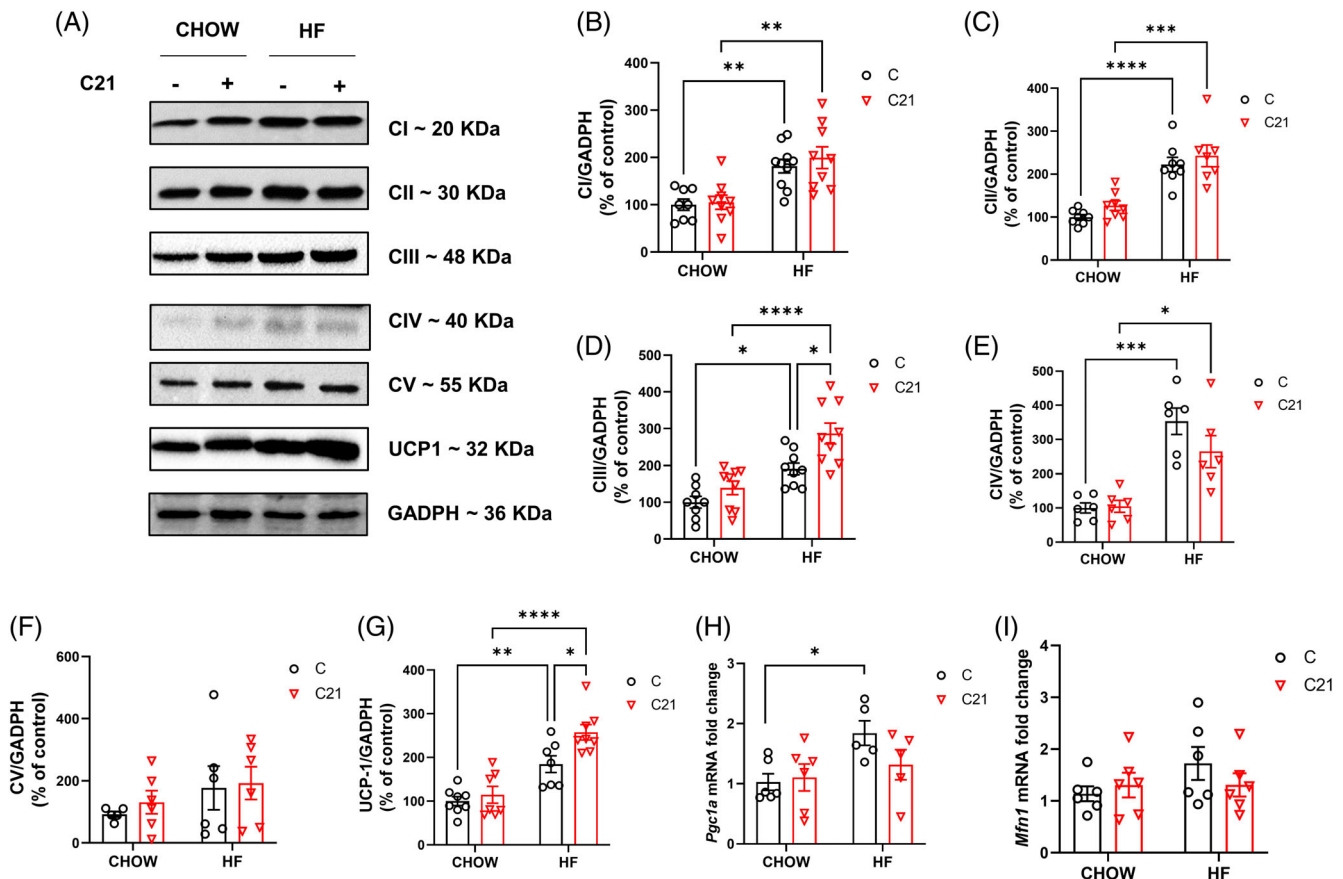


FIGURE 4 C21 promotes mitochondrial uncoupling by increasing complex III and UCP1 in the obese iBAT. (A) iBAT lysates were subjected to Western Blot analysis to quantify the protein complexes of the ETC, ATP synthase and UCP1 ($n = 8$). Relative quantification of complex I (B), complex II (C), complex III (D), complex IV (E), complex V or ATP synthase (F), and UCP1 (G). GAPDH levels were used as a loading control and the relative quantification of the Chow group was set as 100%. (H) mRNA relative levels of markers of mitochondrial biogenesis *Pgc1a* (I) and *Mfn1* (J) ($n = 6$). The relative expression of the Chow group was set as 1. Results were normalized using the expression of *Gapdh* and *Hprt* as housekeeping genes. Data are represented as mean \pm SEM. * $p < 0.05$, ** $p < 0.01$, *** $p < 0.001$, **** $p < 0.0001$. C21, compound 21; ETC: electron transport chain; iBAT: interscapular brown adipose tissue; UCP1: uncoupling protein 1.

Finally, the expression of key enzymes and transcription factors in oxidative metabolic pathways was measured. No differences were observed among any of the four groups in the expression of genes related to lipid uptake (*Cd36*, *Ldlr*), intracellular lipid transport (*Fabp4*), or lipid oxidation (*Ppara*, *Hsl*, or *Cpt1b*) (Supporting Information Figure S1).

3.5 | C21 exerts anti-inflammatory and antioxidant roles in the iBAT of obese mice

Next, we wanted to assess if the enhanced metabolic performance observed in HF-C21 animals was related to the anti-inflammatory and antioxidant properties of C21. To assess iBAT inflammation, tissue sections were immunostained with anti-CD68 antibody, a macrophage marker. When comparing the images from the four study

groups, HFD mice showed an increase in stained area compared to CHOW animals, indicating higher macrophage infiltration. However, C21 treatment in obese animals was able to revert the infiltration of macrophages within the tissue (Figure 5A,B). In accordance with these results, the expression of the chemoattractant cytokine *Mcp-1* was four-fold higher in the HF mice but reduced to basal levels in HF-C21 animals (Figure 5C). The expression of proinflammatory cytokines *Il-1 β* and *Il-6* followed a similar pattern: higher relative levels of mRNA were found in the iBAT of HF mice in comparison to CHOW, but they were normalized in HF-C21 mice. (Figure 5D,E), confirming the anti-inflammatory properties of C21 administration in the iBAT of obese mice. The activity of the antioxidant enzyme SOD was also increased in HF-fed animals, while restored to basal levels in the HF-C21, suggesting that C21 also ameliorates the oxidative status of the obese iBAT (Figure 5F).

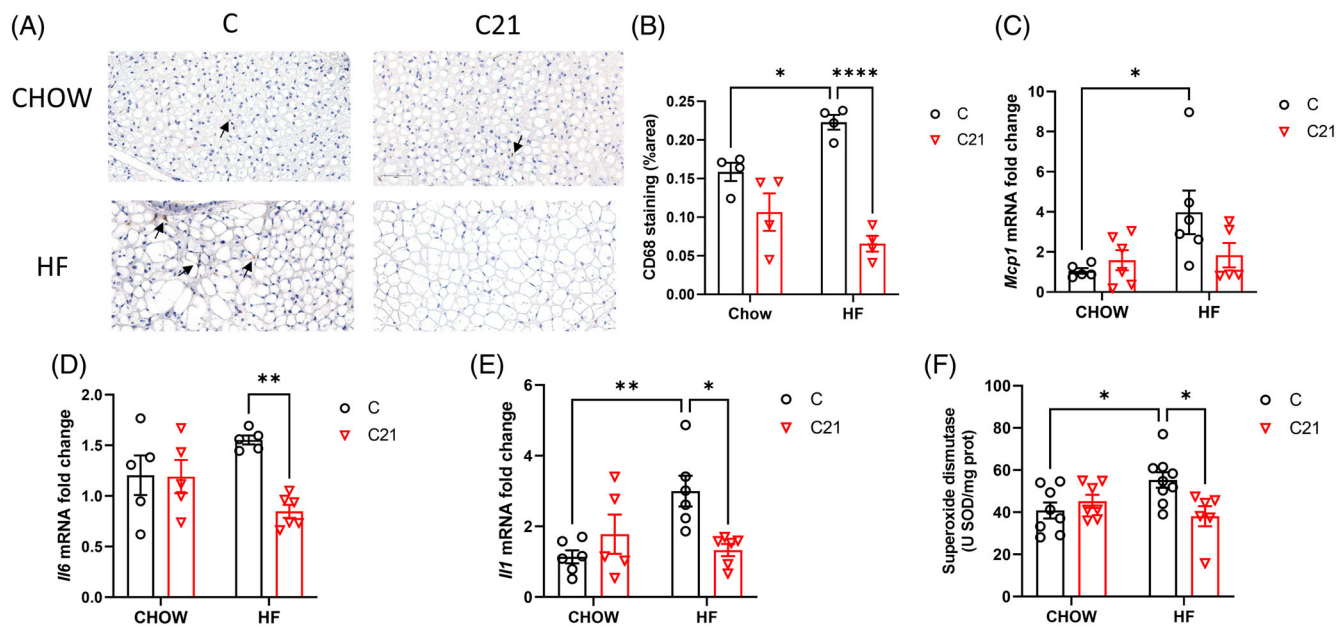


FIGURE 5 C21-mediated AT2R activation exerts anti-inflammatory and antioxidant properties in the iBAT of obese mice. (A) Representative images of immunohistochemical localization of CD68. Black arrows point at positive-stained macrophages. The stained area was quantified from at least three independent fields from each slide and macrophage infiltration was expressed as percentage of total area (B) ($n = 4$). mRNA relative expression of *Mcp1* (C), *Il-6* (D), and *Il-1* (E). The relative expression of the Chow group was set as 1. Results were normalized using the expression of *Gapdh* and *Hprt* as housekeeping genes. (F) Specific activity of SOD in iBAT lysates ($n = 8$). Data are represented as mean \pm SEM. * $p < 0.05$, ** $p < 0.01$, **** $p < 0.0001$. AT2R: angiotensin II type 2 receptor; C21, compound 21; iBAT: interscapular brown adipose tissue; SOD: superoxide dismutase.

3.6 | AT2R activation potentiates the ETC and UCP1 in the obese tPVAT

Finally, to evaluate if the beneficial actions of AT2R activation by C21 in obesity could be extended to other brown adipose depots, we analyzed the adipose tissue that surrounds the thoracic aorta. The histological analysis revealed a higher number of large lipid droplets within the tPVAT of the HF animals compared to CHOW, but they were not as frequent in the HF-C21 mice (Figure 6A, left). However, the differential fat accumulation did not influence tPVAT weight in any of the four groups (Figure 6B).

Macrophage infiltration was observed in the tPVAT of the four experimental groups (Figure 6A, right). The relative quantification of the CD68-positive stained area revealed no differences among the groups (% stained area: CHOW = 0.216 ± 0.065 vs. HF = 0.292 ± 0.058 vs. HF-C21 = 0.275 vs. 0.059). However, mRNA levels of the proinflammatory cytokine *Il1* showed a non-significant upregulation trend in the HF group compared to CHOW (2.5-fold increase; $p = 0.056$), that was restored to basal levels in the HF-C21 animals (Figure 6C).

Unlike in the iBAT, we did not observe an increase in the components of the ETC of the tPVAT of HF animals. No differences were found between the HF and CHOW

group in the protein levels of any of the respiratory complexes (Figure 6D–I). However, the treatment with C21 in HF animals promoted an increase in the protein levels of complexes I and II in comparison to the HF group (Figure 6E,F) and complex IV when compared to CHOW-C21 (Figure 6H). Finally, HF induced a significant upregulation of UCP1 protein levels independently of the C21 treatment when compared to their counterparts (Figure 6J).

4 | DISCUSSION

BAT activation has arisen as a promising therapeutic tool in the treatment of metabolic diseases in the last decade. Beta-adrenergic stimulation has proven to successfully increase energy expenditure and restore metabolic homeostasis, but the therapeutic window is dangerously close to the toxic dose that cause cardiovascular side effects.²⁸ Considering that CVDs are a common feature in patients with obesity, unraveling new mechanisms of BAT activation may open the door to the discovery of safer therapies. Since the protective arm of the RAS exerts cardioprotective properties, in this report, we employed a diet-induced obesity model to evaluate the activation of the BAT thermogenic program using C21, a specific agonist of the AT2R.

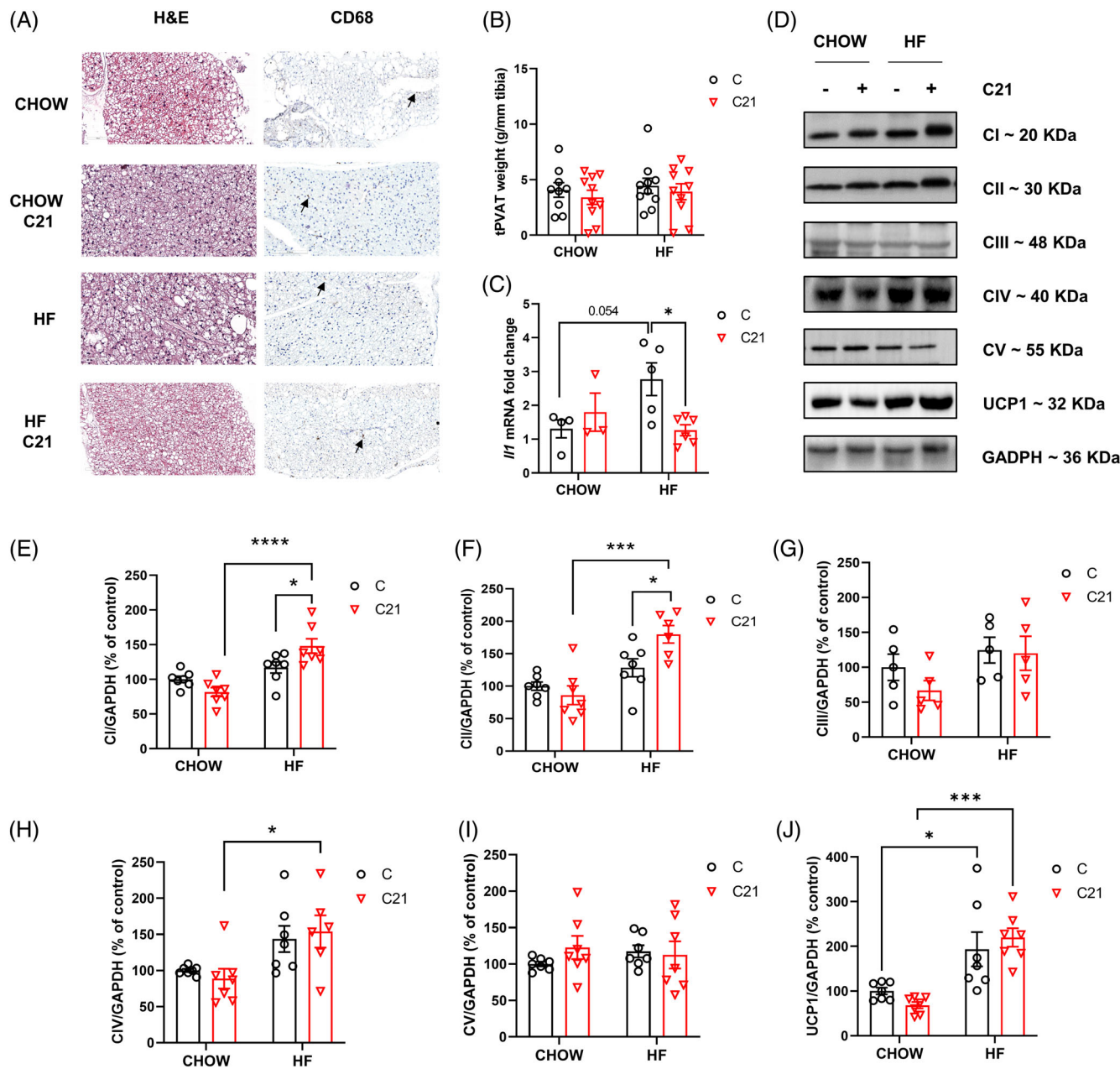


FIGURE 6 C21 boosts the electron transport chain and reduces inflammatory markers in the tPVAT of obese mice. (A) Representative images of hematoxylin/eosin stain of paraffin-embedded iBAT slices (left) and representative images of immunohistochemical localization of CD68. Black arrows point at positive-stained macrophages (right). (B) tPVAT weight, expressed as mg/mm tibia. (C) mRNA relative expression of *Il-1*. The relative expression of the Chow group was set as 1. Results were normalized using the expression of *Gapdh* and *Hprt* as housekeeping genes. (D) tPVAT lysates were subjected to Western Blot analysis to quantify the protein complexes of the ETC, ATP synthase and UCP1 ($n = 5-7$). Relative quantification of complex I (E), complex II (F), complex III (G), complex IV (H), complex V or ATP synthase (I), and UCP1 (J). GAPDH levels were used as a loading control and the relative quantification of the Chow group was set as 100%. Data are represented as mean \pm SEM. * $p < 0.05$, *** $p < 0.001$, **** $p < 0.0001$. C21, compound 21; ETC: electron transport chain; iBAT: interscapular brown adipose tissue; tPVAT: thoracic perivascular adipose tissue; UCP1: uncoupling protein 1.

The benefits of activating iBAT to treat metabolic diseases have been widely described. Cold activation or adrenergic stimulation, among others, have shown to reduce dyslipidemia or insulin resistance.^{29,30} In our model, C21-mediated activation of iBAT in HFD-fed mice

did not modify body mass, but successfully reduced circulating insulin levels. In addition, previous reports from our group in these animals showed that C21 preserves the endothelial function in thoracic and abdominal aorta from obese mice,^{26,27} demonstrating a role in

cardiovascular protection. According to our results, C21 enhances BAT activity in obese mice by (i) enhancing thermogenesis via ETC and UCP1 upregulation; (ii) increasing BAT mass through a promotion of cell differentiation, and (iii) improving BAT function through a reduction in inflammation and oxidative stress.

A defective mitochondrial ETC and oxidative phosphorylation (OxPhos) are hallmark features of metabolic diseases such as diabetes and obesity. In humans, a lower OxPhos capacity in WAT has been linked to higher body mass index.^{31,32} In BAT, however, due to its key role in thermogenesis, the ETC is mostly uncoupled from energy production via UCP1. As a mechanism of adaptation to energy-rich diets, substrate oxidation, ETC, and thermogenesis are increased in the BAT of HF diet-fed animals in an UCP1-dependent manner.^{33,34} We have previously described how 20 weeks of HF diet feeding produced a two-fold increase in oxygen consumption in the iBAT, together with an increase in complex III and UCP-1 protein levels.²³ Similarly, in this study, 6 weeks of HF diet were sufficient to promote this adaptative thermogenesis, as it was found to increase markers of mitochondrial biogenesis, protein levels of the four respiratory complexes and UCP1. Accordingly, no differences were found in complex V (ATP synthase), confirming that the electrochemical gradient generated by the ETC will be mostly dedicated to thermogenesis and not ATP synthesis, as we also observed in the *in vitro* model. Furthermore, the main finding of this study is that the concomitant administration of HFD with C21, a selective AT2R agonist, lead to a greater increase in iBAT mass, respiratory complex III, and UCP1. These results expand previous observations where intraperitoneal administration of C21 for 2 weeks was able to induce iBAT thermogenesis in lean animals.²⁴ In another study, 2 weeks of C21 treatment also increased UCP1 protein levels and body temperature in HFD-fed animals.³⁵

The discovery of the endocrine capacity of the BAT revealed an important regulatory role that spans beyond the classic view as a thermogenic organ. Through batokines,⁸ lncRNA,³⁶ or extracellular vesicles,³⁷ BAT influences cardiac, hepatic, or brain function, among others.^{10,11} Thus, other anatomical regions rich in brown-like adipocytes other than iBAT could participate in the regulation of the physiology of nearby organs. For instance, the adipose tissue that surrounds the thoracic portion of the aorta, known as tPVAT presents brown adipocytes and participates in the regulation of the vascular function by releasing anticontractile vasoactive substances such as the adipocyte-derived relaxing factor (ADRF), angiotensin 1–7, or H₂O₂.³⁸ Likewise iBAT, tPVAT can be metabolically induced by cold, adrenergic agonists, or HFD.^{39–41} In our work, HFD did not modify

tPVAT mass or ETC complex protein levels. Intriguingly, C21 treatment in HFD-fed animals increased complexes I, II, IV, and UCP1, which reflects an increased substrate oxidation and a later dedication of the released energy as heat rather than ATP synthesis. Potentiating the brown characteristics of PVAT has been proposed to exert protective effects in the aorta.^{12,42} In fact, using a similar methodological approach, we have already described the beneficial effects of AT2R activation by C21 in the thoracic aorta of obese animals.⁴³ C21 prevented the development of obesity-induced endothelial dysfunction by stimulating NO release through PKA/p-eNOS and AKT/p-eNOS pathways. However, in light of the results presented in the current report, we should not discard the contribution of the enhanced activity of tPVAT.

In fact, it is attractive to speculate that AT2R-mediated NO release could be considered as a direct inductor of BAT differentiation and activity. It has been reported that systemic eNOS ablation in mice resulted in the loss of BAT mass.⁴⁴ Recent studies support the role of NO to enhance the thermogenic activity of BAT.^{45,46} In addition, NO could increase brown adipocyte differentiation by stimulating the solubilized guanylate cyclase/PKGI α (cGMP protein-dependent kinase I α)/GSK3 β (glycogen synthase kinase 3 β) pathways (Supporting Information Figure S2). Interestingly, AT2R agonists have demonstrated to activate the same pathway.⁴⁷ This mechanism of brown adipocyte differentiation could explain the observation of Than and colleagues,²⁴ who described how Ang II-induced AT2R activation promoted brown adipocyte proliferation and adipogenesis *in vitro*.

These results are consistent with our findings, where C21-induced AT2R activation increased adipogenesis and the mitochondrial oxygen consumption dedicated to thermogenesis in brown adipocytes differentiated *in vitro*. Our results demonstrate that this activation is AT2R specific and dose-dependent. Stimulating brown preadipocytes with micromolar concentrations of C21 resulted in an ablation of their ability to differentiate. At this range of concentrations, C21 loses its specificity and binds to AT1R, inhibiting differentiation. However, when nanomolar concentrations of C21 were used, it binds exclusively to AT2R (K_i AT2R = 0.4 nM vs. K_i AT1R > 10 μ M) promoting brown adipocyte differentiation and mitochondrial respiration due to H⁺ leak, which was confirmed with the cotreatment in the presence of the corresponding AT1R and AT2R inhibitors. Overall, these *in vitro* evidence could explain the increase in the iBAT mass, ETC, and UCP1 levels that we observed in our animal model.

We have previously shown that obesity promotes oxidative stress and inflammation in the iBAT of HFD-fed



mice.²³ In fact, time-course microarrays revealed increased immune trafficking after 8 weeks of HFD.⁴⁸ The overactivation of the deleterious branch of the RAS, including Ang II circulating levels and AT1R expression, has been reported in obesity^{24,49} and can contribute to the oxidative and inflammatory status that we observed in the BAT of the obese animals. The administration of C21 was able to reduce AT1R levels while maintaining AT2R. Due to the existing negative cross-regulation between AT1R and AT2R, the administration of C21 could prevent the inflammation and oxidative stress mediated by AT1R overactivation. Thus, indirectly, the amelioration of inflammation and oxidative stress could also explain the enhanced function of the BAT, since both processes have proved to alter mitochondrial structure and function.^{39,50,51}

5 | CONCLUSION

In this report, we demonstrate that the activation of the reparative branch of the RAS increases the thermogenic program of the obese BAT by (1) increasing ETC complexes and UCP1 protein levels; (2) promoting cell differentiation, resulting in increased BAT mass, and (3) improving BAT physiology by decreasing the inflammatory and oxidative state. Therefore, better glucose homeostasis and vascular function were achieved. Since the administration of C21 was concomitant to the dietary intervention, further studies should be carried out to confirm if C21 could be a potential candidate in the treatment rather than in the prevention of obesity-related metabolic alterations.

AUTHOR CONTRIBUTIONS

Conceptualization: Martín Alcalá, Marta Viana, Marta Gil-Ortega, and Beatriz Somoza; **Methodology:** Martín Alcalá, Marta Viana, Marta Gil-Ortega, and Beatriz Somoza; **Investigation:** Fabiola Alvarez-Gallego, Raquel González-Blázquez, María Calderón-Dominguez, Javier Moratinos, Virginia Garcia-Garcia, Paloma Fernández, Daniel González-Moreno, and Martín Alcalá; **Resources:** Martín Alcalá, Marta Viana, Marta Gil-Ortega, and Beatriz Somoza; **Data curation:** Fabiola Alvarez-Gallego, Raquel González-Blázquez, María Calderón-Dominguez, Javier Moratinos, Virginia Garcia-Garcia, Paloma Fernández, and Daniel González-Moreno; **Writing—original draft preparation:** Fabiola Alvarez-Gallego and Martín Alcalá; **Writing—review and editing:** Raquel González-Blázquez, Marta Viana, Marta Gil-Ortega, Beatriz Somoza, and María Calderón-Dominguez; **Visualization:** Fabiola Alvarez-Gallego, Raquel González-Blázquez, and Martín Alcalá; **Supervision:** Martín Alcalá,

Marta Viana, Marta Gil-Ortega, and Beatriz Somoza. **Funding acquisition:** Martín Alcalá, Marta Viana, Marta Gil-Ortega, and Beatriz Somoza. All authors have read and agreed to the published version of the manuscript.

ACKNOWLEDGMENTS

This work was supported by Fundación Universitaria San Pablo CEU—Banco Santander (FUSP-PPC-19-C5B625BA to Marta Viana and FUSP-BS-PPC-USP03/2017 to Marta Gil-Ortega) and Ministerio de Ciencia e Innovación (PID2020-114343GA-I00 to Martín Alcalá).

DATA AVAILABILITY STATEMENT

The data that support the findings of this study are available from the corresponding author upon reasonable request.

ORCID

Marta Viana  <https://orcid.org/0000-0003-4718-4145>

Martín Alcalá  <https://orcid.org/0000-0003-4678-8860>

REFERENCES

1. Cannon B, Nedergaard J. Brown adipose tissue: function and physiological significance. *Physiol Rev.* 2004;84(1):277–359.
2. Enerbäck S, Jacobsson A, Simpson EM, Guerra C, Yamashita H, Harper ME, et al. Mice lacking mitochondrial uncoupling protein are cold-sensitive but not obese. *Nature.* 1997;387:90–4.
3. Becher T, Palanisamy S, Kramer DJ, Eljalby M, Marx SJ, Wibmer AG, et al. Brown adipose tissue is associated with cardiometabolic health. *Nat Med.* 2021;27(1):58–65.
4. Verkerke ARP, Kajimura S. Oil does more than light the lamp: the multifaceted role of lipids in thermogenic fat. *Dev Cell.* 2021;56(10):1408–16.
5. Nicholls D, Locke R. Reviews in brown fat. *Physiol Rev.* 1984; 64:3–64.
6. Shamsi F, Wang CH, Tseng YH. The evolving view of thermogenic adipocytes—ontogeny, niche and function. *Nat Rev Endocrinol.* 2021;17(12):726–44.
7. Zhou X, Li Z, Qi M, Zhao P, Duan Y, Yang G, et al. Brown adipose tissue-derived exosomes mitigate the metabolic syndrome in high fat diet mice. *Theranostics.* 2020;10(18):8197–210.
8. Gavaldà-Navarro A, Villarroya J, Cereijo R, Giralt M, Villarroya F. The endocrine role of brown adipose tissue: an update on actors and actions. *Rev Endocr Metab Disord.* 2022; 23(1):31–41.
9. Pinckard KM, Shettigar VK, Wright KR, Abay E, Baer LA, Vidal P, et al. A novel endocrine role for the BAT-released Lipokine 12,13-diHOME to mediate cardiac function. *Circulation.* 2021;143(2):145–59.
10. Han F, Kan C, Wu D, Kuang Z, Song H, Luo Y, et al. Irisin protects against obesity-related chronic kidney disease by regulating perirenal adipose tissue function in obese mice. *Lipids Health Dis.* 2022;21(1):115.
11. Ruan CC, Kong LR, Chen XH, Ma Y, Pan XX, Zhang ZB, et al. A2A receptor activation attenuates hypertensive cardiac

- remodeling via promoting Brown adipose tissue-derived FGF21. *Cell Metab.* 2018;28(3):476–489.e5.
12. Gil-Ortega M, Stucchi P, Guzmán-Ruiz R, Cano V, Arribas S, González MC, et al. Adaptive nitric oxide overproduction in perivascular adipose tissue during early diet-induced obesity. *Endocrinology.* 2010;151(7):3299–306.
 13. Adachi Y, Ueda K, Nomura S, Ito K, Katoh M, Katagiri M, et al. Beiging of perivascular adipose tissue regulates its inflammation and vascular remodeling. *Nat Commun.* 2022;13(1):5117.
 14. Cypess AM, Weiner LS, Roberts-Toler C, Elia EF, Kessler SH, Kahn PA, et al. Activation of human brown adipose tissue by a β 3-adrenergic receptor agonist. *Cell Metab.* 2015;21(1):33–8.
 15. Finlin BS, Memetimin H, Zhu B, Confides AL, Vekaria HJ, El Khouli RH, et al. The β 3-adrenergic receptor agonist mirabegron improves glucose homeostasis in obese humans. *J Clin Invest.* 2020;130(5):2319–31.
 16. Szentirmai E, Kapas L. The role of the brown adipose tissue in β 3-adrenergic receptor activation-induced sleep, metabolic and feeding responses. *Sci Rep.* 2017;7(1):958.
 17. Blondin DP, Nielsen S, Kuipers EN, Severinsen MC, Jensen VH, Miard S, et al. Human brown adipocyte thermogenesis is driven by β 2-AR stimulation. *Cell Metab.* 2020;32(2):287–300.e7.
 18. O'Mara AE, Johnson JW, Linderman JD, Brychta RJ, McGehee S, Fletcher LA, et al. Chronic mirabegron treatment increases human brown fat, HDL cholesterol, and insulin sensitivity. *J Clin Invest.* 2020;130(5):2209–19.
 19. Kimura H, Nagoshi T, Yoshii A, Kashiwagi Y, Tanaka Y, Ito K, et al. The thermogenic actions of natriuretic peptide in brown adipocytes: the direct measurement of the intracellular temperature using a fluorescent thermoprobe. *Sci Rep.* 2017;7(1):12978.
 20. Saito M, Matsushita M, Yoneshiro T, Okamatsu-Ogura Y. Brown adipose tissue, diet-induced thermogenesis, and Thermogenic food ingredients: from mice to men. *Front Endocrinol (Lausanne).* 2020;11:222.
 21. Karnik SS, Unal H, Kemp JR, Tirupula KC, Eguchi S, Vanderheyden PML, et al. Angiotensin receptors: interpreters of pathophysiological angiotensinergic stimulus. *Pharmacol Rev.* 2015;67(4):754–819.
 22. Tyurin-Kuzmin PA, Kalinina NI, Kulebyakin KY, Balatskiy AV, Sysoeva VY, Tkachuk VA. Angiotensin receptor subtypes regulate adipose tissue renewal and remodeling. *FEBS J.* 2020;287(6):1076–87.
 23. Alcalá M, Calderon-Dominguez M, Bustos E, Ramos P, Casals N, Serra D, et al. Increased inflammation, oxidative stress and mitochondrial respiration in brown adipose tissue from obese mice. *Sci Rep.* 2017;7(1):16082.
 24. Than A, Xu S, Li R, Leow MS, Sun L, Chen P. Angiotensin type 2 receptor activation promotes browning of white adipose tissue and brown adipogenesis. *Signal Transduct Target Ther.* 2017;2:17022.
 25. Morimoto H, Mori J, Nakajima H, Kawabe Y, Tsuma Y, Fukuhara S, et al. Angiotensin 1–7 stimulates brown adipose tissue and reduces diet-induced obesity. *Am J Physiol Endocrinol Metab.* 2018;314(2):E131–8.
 26. González-Blázquez R, Alcalá M, Cárdenas-Rebollo JM, Viana M, Steckelings UM, Boisvert WA, et al. AT2R stimulation with C21 prevents arterial stiffening and endothelial dysfunction in the abdominal aorta from mice fed a high-fat diet. *Clin Sci (Lond).* 2021;135(24):2763–80.
 27. González-Blázquez R, Alcalá M, Fernández-Alfonso MS, Steckelings UM, Paz Lorenzo M, Viana M, et al. C21 preserves endothelial function in the thoracic aorta from DIO mice: role for AT2, mas and B2 receptors. *Clin Sci (Lond).* 2021;135(9):1145–63.
 28. Loh RKC, Formosa MF, La Gerche A, Reutens AT, Kingwell BA, Carey AL. Acute metabolic and cardiovascular effects of mirabegron in healthy individuals. *Diabetes Obes Metab.* 2019;21(2):276–84.
 29. Chondronikola M, Volpi E, Børsheim E, Porter C, Annamalai P, Enerbäck S, et al. Brown adipose tissue improves whole-body glucose homeostasis and insulin sensitivity in humans. *Diabetes.* 2014;63(12):4089–99.
 30. Larsen TM, Toubro S, Van Baak MA, Gottesdiener KM, Larson P, Saris WHM, et al. Effect of a 28-d treatment with L-796568, a novel β 3-adrenergic receptor agonist, on energy expenditure and body composition in obese men. *Am J Clin Nutr.* 2002;76(4):780–8.
 31. Dahlman I, Forsgren M, Sjögren A, Nordström EA, Kaaman M, Näslund E, et al. Downregulation of electron transport chain genes in visceral adipose tissue in type 2 diabetes independent of obesity and possibly involving tumor necrosis factor- α . *Diabetes.* 2006;55(6):1792–9.
 32. Fischer B, Schöttl T, Schempp C, Fromme T, Hauner H, Klingenspor M, et al. Inverse relationship between body mass index and mitochondrial oxidative phosphorylation capacity in human subcutaneous adipocytes. *Am J Physiol Endocrinol Metab.* 2015;309(4):E380–7.
 33. Mackert O, Wirth EK, Sun R, Winkler J, Liu A, Renko K, et al. Impact of metabolic stress induced by diets, aging and fasting on tissue oxygen consumption. *Mol Metab.* 2022;1:64.
 34. von Essen G, Lindsund E, Cannon B, Nedergaard J. Adaptive facultative diet-induced thermogenesis in wild-type but not in UCP1-ablated mice. *Am J Physiol Endocrinol Metab.* 2017;313(5):E515–27.
 35. Nag S, Patel S, Mani S, Hussain T. Role of angiotensin type 2 receptor in improving lipid metabolism and preventing adiposity. *Mol Cell Biochem.* 2019;461(1–2):195–204.
 36. Corral A, Alcalá M, Carmen Duran-Ruiz M, Arroba AI, Ponce-Gonzalez JG, Todorčević M, et al. Role of long non-coding RNAs in adipose tissue metabolism and associated pathologies. *Biochem Pharmacol.* 2022;1:206.
 37. Camino T, Lago-Baameiro N, Sueiro A, Bravo SB, Couto I, Santos FF, et al. Brown adipose tissue sheds extracellular vesicles that carry potential biomarkers of metabolic and thermogenesis activity which are affected by high fat diet intervention. *Int J Mol Sci.* 2022;23(18):10826.
 38. Fernández-Alfonso MS, Somoza B, Tsvetkov D, Kuczanski A, Dashwood M, Gil-Ortega M. Role of perivascular adipose tissue in health and disease. *Compr Physiol.* 2018;8(1):23–59.
 39. Mestres-Arenas A, Villarroya J, Giralt M, Villarroya F, Peyrou M. A differential pattern of batokine expression in perivascular adipose tissue depots from mice. *Front Physiol.* 2021;4:12.
 40. Mirbolooki MR, Constantinescu CC, Pan ML, Mukherjee J. Quantitative assessment of brown adipose tissue metabolic



- activity and volume using 18F-FDG PET/CT and β 3-adrenergic receptor activation. *EJNMMI Res.* 2011;1(1):1–11.
41. Chang L, Villacorta L, Li R, Hamblin M, Xu W, Dou C, et al. Loss of perivascular adipose tissue on peroxisome proliferator-activated receptor- γ deletion in smooth muscle cells impairs intravascular thermoregulation and enhances atherosclerosis. *Circulation.* 2012 Aug 21;126(9):1067–78.
 42. Aldiss P, Davies G, Woods R, Budge H, Sacks HS, Symonds ME. ‘Browning’ the cardiac and peri-vascular adipose tissues to modulate cardiovascular risk. *Int J Cardiol.* 2017;228:265–74.
 43. González-Blázquez R, Alcalá M, Fernández-Alfonso MS, Steckelings UM, Lorenzo MP, Viana M, et al. C21 preserves endothelial function in the thoracic aorta from DIO mice: role for AT2, mas and B2 receptors. *Clin Sci.* 2021;135(9):1145–63.
 44. Nisoli E, Clementi E, Paolucci C, Cozzi V, Tonello C, Sciorati C, et al. Mitochondrial biogenesis in mammals: the role of endogenous nitric oxide. *Science.* 2003;299(5608):896–9.
 45. Sebag SC, Zhang Z, Qian Q, Li M, Zhu Z, Harata M, et al. ADH5-mediated NO bioactivity maintains metabolic homeostasis in brown adipose tissue. *Cell Rep.* 2021;37(7):110003.
 46. Wang CH, Lundh M, Fu A, Kriszt R, Huang TL, Lynes MD, et al. CRISPR-engineered human brown-like adipocytes prevent diet-induced obesity and ameliorate metabolic syndrome in mice. *Sci Transl Med.* 2020;12(558):eaaz8664.
 47. Gao S, Park BM, Cha SH, Park WH, Park BH, Kim SH. Angiotensin AT2 receptor agonist stimulates high stretch induced-ANP secretion via PI3K/NO/sGC/PKG/pathway. *Peptides.* 2013;47:36–44.
 48. McGregor RA, Kwon EY, Shin SK, Jung UJ, Kim E, Park JHY, et al. Time-course microarrays reveal modulation of developmental, lipid metabolism and immune gene networks in intrascapular brown adipose tissue during the development of diet-induced obesity. *Int J Obes (Lond).* 2013;37(12):1524–31.
 49. Saiki A, Ohira M, Endo K, Koide N, Oyama T, Murano T, et al. Circulating angiotensin II is associated with body fat accumulation and insulin resistance in obese subjects with type 2 diabetes mellitus. *Metabolism.* 2009 May;58(5):708–13.
 50. Schönfeld P, Wojtczak L. Brown adipose tissue mitochondria oxidizing fatty acids generate high levels of reactive oxygen species irrespective of the uncoupling protein-1 activity state. *Biochim Biophys Acta.* 2012;1817(3):410–8.
 51. de-Lima-Júnior JC, Souza GF, Moura-Assis A, Gaspar RS, Gaspar JM, Rocha AL, et al. Abnormal brown adipose tissue mitochondrial structure and function in IL10 deficiency. *EBioMedicine.* 2019;39:436–47.

SUPPORTING INFORMATION

Additional supporting information can be found online in the Supporting Information section at the end of this article.

How to cite this article: Alvarez-Gallego F, González-Blázquez R, Gil-Ortega M, Somoza B, Calderón-Dominguez M, Moratino J, et al. Angiotensin II type 2 receptor as a novel activator of brown adipose tissue in obesity. *BioFactors.* 2023. <https://doi.org/10.1002/biof.1981>